

JUNE 1970

CALCULATION OF TRANSITORY REGIMES IN THE COMBUSTION OF  
SOLID FUEL IN A CHANNEL

V. B. Librovich and G. M. Makhviladze

ABSTRACT. Transitory regimes are studies for diffusion combustion occurring when an oxidizer is added from outside the solid fuel composition. Transition from one regime to another is detected by a change in oxidizer consumption. To calculate the transitory regimes a combustion model is used, based on the limiting role of mass transfer. Pressure changes are observed which lag behind changes in oxidizer feed, as well as transitory regimes characterized by formation of dynamic gas waves which cause pressure pulsations alternately reverberating from the front of the channel to the jet. A system of equations describing the static and transitory regimes of combustion, and a finite differential method for integrating them, are proposed. The behavioral laws of the solutions are evaluated.

The case of powders which include oxidizing agents in their composition is examined in [1-8] in research on transitory combustion processes in solid fuels. In [1-3], Ya. B. Zel'dovich gave a theory of dynamic combustion processes in such fuels. One paper [4] is devoted to the numerical calculation of the transitory processes from a stable combustion regime at a single pressure to a stable regime at another pressure by computer. In [5], with the aid of integral correlations, an analytical expression is derived for instantaneous and exponential pressure changes of dynamic powder combustion velocity. The effect of harmonically changing pressure on the combustion rate of powder is studied in [6]. Research was done in [7] on experimental dynamic processes in powder combustion. /33\*

Transitory regimes are examined below for diffusion combustion which takes place when an oxidizer is added from without and is not included in the solid fuel composition. Transition from one regime of combustion to another is given by change in consumption of the oxidizer. Models of combustion for such systems were proposed in [9, 10]. In calculating the

---

\*Numbers in the margin indicate pagination in the foreign text.

transitory regimes a combustion model is used which is based on the limiting role of mass transfer during diffusion combustion [10]. Because of the finite time of discharge of the fuel channel through the jet (when oxidizer feed decreases) or filling up (when oxidizer consumption increases), channel pressure will lag behind changes in oxidizer feed. In addition, transitory regimes are characterized by formation of dynamic gas waves in the channel which cause pressure pulsations, alternately reverberating from the frontal and jet parts of the channel. The combustion rate of solid fuel depends on the mass velocity of gas flow, and therefore burnout of the channel occurs irregularly. A system of equations describing static and transitory regimes of combustion and a finite differential method for integrating it are proposed. The behavioral laws of the solutions obtained are evaluated.

1. Setting Up the Problem. Let the fuel be in the form of a cylindrical cartridge with an axial channel of radius  $R$ , through which flows a stream of oxidizer. Axis  $x$  is directed along the symmetrical axis;  $x = 0$  coincides with the beginning of the channel. Its length is  $l$ . The channel is choked with a supersonic jet. We will use the following suppositions for solution of the problem.

1°. Flow is one-dimensional and turbulent along the whole length of the channel. Here we disregard inequalities of flow in transverse directions  $y$  and  $z$ , which can appear as a result of expansion or distortion of the channel walls, erosion of combustion products off the walls, and the results of vibration or fuel passage. The suitability of this hypothesis is supported by the fact that gas motion in a channel has a turbulent character, while turbulence is intensified by the injection of fuel and mass as a result of the chemical combustion reaction taking place along the walls (see 2°). Note that the one-dimensional model supposes complete mixture of oxidizer and fuel products in each channel cross section.

2°. In the channel, diffusion combustion takes place on the walls (this model is evaluated in [10]), i.e., a diffused flame of chemical reaction products rises over the fuel surface from the vaporization of the solid fuel and the gaseous oxidizer washing its surface; it is located within the

boundary layer. Note the distance from the flame to the fuel surface is inversely proportional to the combustion rate [10]. Therefore the proposition made here is valid as long as the oxidizer concentration in the stream is not too small. Actually, as oxidizer concentration decreases (that is, as  $x$  increases), the diffused flame moves away from the solid fuel surface; therefore it is all the more subject to the effect of the turbulent stream. As a result, the flame deforms and becomes tattered; breaks may appear on its surface; then another mechanism of solid fuel demolition begins to play a qualitative role, and that is ablation. Therefore we will consider the channel being not too long, and the Reynolds number (determined by the combustion rate) not very high. Since the flame is distributed in the depth of the boundary layer, we will consider the chemical reaction to be concentrated at the channel walls.

3°. Gas is considered as the ideal constant of molecular weight.

4°. We will also disregard the change of shape and size of the channel in the course of the transition process.

5°. We will disregard the dependence of thermal effect on gas flow parameters, i.e., we will consider the burned fuel layer as instantly changing to the gas flow state.

6°. Gas motion is turbulent by nature, therefore it is natural to disregard phenomena of molecular transfer also.

2. The Equations and Boundary Conditions. Before we write a system of equations, we will show that combustion rate of a solid fuel can be written in the form

$$\dot{m} = B_m a j^n \quad (2.1)$$

Here  $\dot{m}$  is the mass combustion rate of the solid fuel,  $a$  is the relative weight concentration of oxidizer,  $B_m$  and  $n$  are constant values, and  $j$  is the mass velocity of gas flow.

Expression (2.1) can be obtained for combustion rate using the condition of stoichiometric correlation between fuel and oxidizer currents in the diffused flame and calculating the mass transfer coefficient from the critical

connection between Nusselt's diffusion number, Reynolds and Prandtl numbers and the relationship of the rate of gas flowing out from the fuel to the long-term rate of oxidizer flow [10].

For the basic equations we will use the one-dimensional gas-dynamic equations, accounting for heat sources and masses concentrated on the walls. Since the values of gas consumption, its concentration, and also enthalpy will be given in a calculation of the modes at the channel entrance, it is convenient to write the system of equations in dependent variables  $j$ ,  $p$  (gas pressure),  $a$ ,  $H$  (gas enthalpy), using (2.1) for  $m$ .

Introducing the abstract variables (indicated by a prime-')

$$\begin{aligned} j' &= \frac{j}{j_0}, \quad H' = \frac{H}{H_0}, \quad a' = \frac{a}{a_0} \\ x' &= \frac{x}{l}, \quad p' = \frac{p}{j_0 \sqrt{H_0}}, \quad t' = \frac{t \sqrt{H_0}}{l}, \quad Q' = \frac{Q}{H_0} \end{aligned} \quad (2.2)$$

The index below marks the value of a given quantity at cross section  $x = 0$ ,  $Q$  is the effective thermal effect of combustion on the unit weight of the solid fuel,  $t$  is time.

In these variables (the primes are dropped hereafter) the system of equations has the form

/35

$$\frac{\partial w}{\partial t} + \frac{\partial f}{\partial x} = s \quad (2.3)$$

Here  $w$ ,  $f$ , and  $s$  are single-column matrices with the components

$$\begin{aligned} w_1 &= \frac{\gamma p}{(\gamma-1)H}, \quad w_2 = \frac{\gamma p a}{(\gamma-1)H}, \quad w_3 = j \\ w_4 &= \frac{p}{\gamma-1} + \frac{1}{2} \frac{\gamma-1}{\gamma} \frac{j^2 H}{p} \\ f_1 &= j, \quad f_2 = aj, \quad f_3 = p + \frac{\gamma-1}{\gamma} \frac{j^2 H}{p} \\ f_4 &= jH + \frac{1}{2} j \left( \frac{\gamma-1}{\gamma} j \frac{H}{p} \right)^2 \\ s_1 &= v_1 K a j^n, \quad s_2 = -\frac{v_2}{a_0} K a j^n, \quad s_3 = 0, \quad s_4 = Q K a j^n \\ &\left( K = 2 \frac{l}{R} B_m a_0 j_0^{n-1} \right) \end{aligned} \quad (2.4)$$

Here  $\gamma$  is an index of adiabatic gas,  $v_1 = (v_2 + 1)$  a stoichiometric coefficient.

For the solution of this system, three boundary conditions are set at the channel inlet:

$$x = 0, \quad j = h(t), \quad a = 1, \quad H = 1 \quad (2.5)$$

The function  $h(t)$  gives the transition from one combustion mode to another. For  $t < 0$  let a constant dispersion of oxidizer be maintained at the channel entrance, equal to  $a_0 j_0 \pi R^2$ . As a result, a certain stable combustion mode has been established which corresponds to this consumption of oxidizer. The corresponding stable solution found below will serve as the initial condition for solution of the dynamic system of equations (2.3). Then, beginning at moment  $t = 0$ , a sharp change in oxidizer consumption takes place by a factor of several fold, giving function  $h(t)$ , and causing transition to another stationary combustion mode corresponding to the new consumption of oxidizer.

The fourth boundary condition is considered as the presence of a Laval nozzle. If we consider the flow of gas through the nozzle to be quasistable, forming in the gaseous state at the nozzle inlet, then we can use the familiar expression

$$j_l R^2 = A p_l R_*^2 \quad \left[ A = \sqrt{\gamma} \left( \frac{2}{\gamma + 1} \right)^{1/2\alpha} (R^0 T_l)^{-1/2}, \quad \alpha = \frac{\gamma + 1}{\gamma - 1} \right] \quad (2.6)$$

Here  $A$  is the coefficient of gas flow through the nozzle,  $R^0$  is a gas constant,  $T$  is the temperature in the gas flow,  $R_*$  is the radius of the critical nozzle cross section, subscript  $l$  is the value of the given quantity in cross section  $x = l$ . Isolating the temperature function in (2.6) and transforming to the abstract variable, we have

$$x = 1, \quad p_l = \frac{1}{\alpha} j_l H_l^{1/2} \quad \left( \alpha = \frac{\gamma}{(\gamma - 1)^{1/2}} \left( \frac{2}{\gamma + 1} \right)^{1/2\alpha} \left( \frac{R_*}{R} \right)^2 \right) \quad (2.7)$$

3. Solution of the Stable Combustion Problem in the Fuel Channel. We will find the stable solution of the system of equations (2.3) with boundary conditions (2.5) and (2.7). (In this case  $h(t) \equiv 1$ ). Omitting the products of  $t$  in (2.3) and combining the last three equations with the first, we obtain the function  $p$ ,  $H$ ,  $a$  of  $j$ ,  $p_0$  and of the boundary conditions for  $x = 0$ .

/36

$$a = \frac{1}{j} \left[ 1 - \frac{v_2}{v_1 a_0} (j-1) \right], \quad H = \frac{\gamma p}{(\gamma-1)j^2} (\beta - p) \quad \left( \beta = p_0 + \frac{\gamma-1}{\gamma p_0} \right) \quad (3.1)$$

$$p = \frac{1}{\gamma+1} \left\{ \beta + \left[ \gamma^2 \beta^2 + 2(\gamma^2-1)j \left[ \frac{Q}{v_1} (1-j) - 1 - \frac{1}{2}(\beta - p_0)^2 \right] \right]^{1/2} \right\}$$

Substituting the expression for  $a$  in the first stable equation of system (2.3), we obtain a differential equation describing the change of gas flow along the channel axis:

$$\frac{dj}{dx} = v_1 K j^{n-1} \left( 1 - \frac{v_2(j-1)}{v_1 a_0} \right) \quad (3.2)$$

For random values it can only be integrated numerically<sup>1</sup>, but we can obtain analytical expressions for  $n = 0.5$  and  $n = 1.0$ , which majorizes the real function  $j = j(x)$  for  $0.5 < n < 1$  above and below. These expressions are given as

$$j = 1 + \frac{v_1 a_0}{v_2} \left[ 1 - \exp \left( - \frac{v_2}{a_0} K x \right) \right] \quad (n=1) \quad (3.3)$$

$$2(d^2 - 1) \left[ 1 - \sqrt{j} + \frac{d}{2} \ln \frac{(d + \sqrt{j})(d-1)}{(d - \sqrt{j})(d+1)} \right] = v_1 K x \quad (n=0.5) \quad (3.4)$$

$$d = \left( 1 + \frac{v_1 a_0}{v_2} \right)^{1/2}$$

<sup>1</sup>For numerical calculation, the Eulerian method was used. The interval of values from 0 to 1 was divided into 100 parts, so that  $x_i = i\Delta x$ , where  $\Delta x = 0.01$ ,  $i = 0, 1, 2, \dots, 100$ . The terminal differential equation corresponding to differential equation (3.2) has the form

$$j(x_i + \Delta x) = j(x_i) + \Delta x \left( v_1 + \frac{v_2}{a_0} \right) K [j(x_i)]^{n-1} - \Delta x \frac{v_2}{a_0} K [j(x_i)]^n$$

This equation allows calculation of flow  $j$  for each  $x$ . The results of calculation are given in Figure 1. Curve 3 was obtained by numerical calculation for  $n = 0.76$ , curves 6 and 7 were plotted for  $n = 1$  and  $n = 0.5$  (the remaining parameters are identical). From the Figure we see that the static solution can be obtained with good accuracy from (3.3) and (3.4).

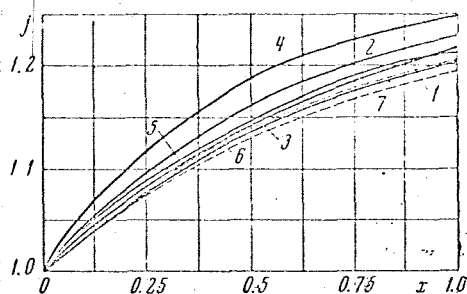


Figure 1.

From (3.2) we can determine the quantity  $j_L$ . Writing the second and third equation of the system (3.1) where  $x = L$  and using the boundary condition (2.7), we obtain a system of equations from which we find the function of the pressure quantity at the channel inlet  $p_0$  of  $j_L$

$$p_0^2 = \frac{\gamma-1}{\gamma^2} \left[ \sigma - \varepsilon + \left( \sigma^2 - 2\sigma\varepsilon + \frac{\gamma-1}{\gamma} \varepsilon \right)^{1/2} \right] \quad (3.5)$$

$$\sigma = 1 + \frac{Q}{v_1} (j_L - 1), \quad \varepsilon = \kappa^2 \frac{\gamma-1}{\gamma L} \left[ 2 + \left( \frac{\gamma-1}{\gamma} \kappa \right)^2 \right] \left( 1 + \frac{\gamma-1}{\gamma} \kappa^2 \right)^{-2}$$

Now from (3.1) it is easy to find all the remaining functions.

In calculating, we used different values of abstract parameters which enter into the equations and boundary conditions.

1°. Let  $\gamma = 1.276$ ,  $\kappa = 0.3182$ ,  $Q = 33.33$ ,  $a_0 = 0.22$ ,  $n = 0.76$ ,  $v_1 = 4.43$ . With these values calculation was made for  $K_1 = 0.0906$ ,  $K_2 = 0.0822$ , and  $K_3 = 0.1070$ .

Parameter  $K_1$  corresponds to twice the consumption of oxidizer at the channel inlet than does parameter  $K_3$ , and parameter  $K_2$  for 1.5 times the oxidizer consumption of  $K_1$ , (other parameters are identical).

/37

The station solutions obtained are illustrated in Figure 1 and are shown by numbers 1, 2 and 3 corresponding to  $K$ . Point  $x = 1.0$  on the axis of the abscissa corresponds to the channel end.

Note that towards the end of the channel for case 1, there is a flow increase of 21.3%. The quantity of oxidizer carried out with the gas flow through the nozzle is 20.7% of the quantity of oxidizer entering into the channel. From the third equation of the basic system (2.3) we have

$$p_L = p_0 (1 + \gamma M_0^2) / (1 + \gamma M_L^2) \quad (3.6)$$



where  $M$  is the Mach number. Inasmuch as motion in the channel is substantially subsonic, ( $M_0 = 0.08$ ,  $M_L = 0.13$  for case 1), pressure along the channel axis is insignificant:  $p_0 = 5.66$  and falls at the end of the channel to 1.5%.

Enthalpy of gas in this case increases by 114% toward the final cross section of the channel. Thus the relative increase of mass flow is considerably less than the relative increase in gas enthalpy.

Finally, we introduce the values for the time the gas proceeds along the channel (or time for the fuel channel to empty)  $t_1 = 12.5$ , and time of sound interference dispersion  $t_2 = 1.4$  (for all three cases, these characteristic times are practically identical).

2°. Suppose  $\gamma = 1.283$ ,  $\kappa = 0.5141$ ,  $Q = 36.50$ ,  $a_0 = 0.21$ ,  $n = 0.76$ ,  $v_1 = 4.43$ . These parameters were used in calculation for  $K_4 = 0.1447$  and  $K_5 = 0.0935$ .

Parameter  $K_5$  corresponds to a consumption of oxidizer at the channel inlet 6.17 times greater than  $K_4$  (the other parameters being the same).

The solution for these two cases is entered in Figure 1 and shown by numbers 4 and 5 corresponding to  $K$ . The regular behavior of the solution is the same as in case 1°. In this case  $t_1 = 7.1$ , and  $t_2 = 1.2$ .

4. Integration of the Dynamic Equations. The dynamic problem was solved numerically using the two-sloped plain differential system of second-order accuracy proposed in [11]. Artificial viscosity (needed for automatic calculation of skips) appears in (4.1) in implicit form because approximation of the differential equations is terminal-differential. All values are calculated at the lattice corners  $x_i = i\Delta x$ ,  $i = 0, \dots, 100$ ;  $t = m\Delta t$ ,  $m = 0.1\dots$  Writing out this diagram,

$$w_{i+1/2}\left(t + \frac{\Delta t}{2}\right) = \frac{w_{i+1}(t) + w_i(t)}{2} - \frac{\Delta t}{2\Delta x} [f_{i+1}(t) - f_i(t)] + \frac{\Delta t}{2} s_{i+1/2}(t) \quad (4.1)$$

$$w_i(t + \Delta t) = w_i(t) - (\Delta t/\Delta x) [f_{i+1/2}(t + 1/2 \Delta t) - f_{i-1/2}(t + 1/2 \Delta t)] + \Delta t s_i(t + 1/2 \Delta t)$$

All values are calculated first at the semi-integral stage at the moment  $t + 1/2 \Delta t$  for the system at the first order of accuracy (the first of equations (4.1)) and then at the moment  $t + \Delta t$  using the values at the semi-integral level, so that the resultant system (4.1) has second-order accuracy.

In order to improve the quality of calculation, a smooth (exponential) transition to the new consumption of oxidizer is used in place of a sharp drop, i.e.,

$$h(t) = k + (1 - k) e^{-\lambda m \Delta t} \quad (4.2)$$

Here  $k$  is the final gas flow at the channel inlet (the initial flow /38 equals 1) in the transitory regime;  $\lambda$  is selected so that the new consumption of oxidizer is sufficiently and rapidly established. Calculations were made for three cases. Studies were made for  $k = 6.17$ , 0.5 and 1.5.

In order that the selected differential system would be stable (i. e., so that small errors arising in the calculation process would not multiply), correlation of steps in time and coordinate had to satisfy the Courant-Friedrichs-Levi stability criteria, i.e.,

$$\max_x (|u| + c) \Delta t / \Delta x \leq 1$$

The step along  $x$  was selected, as in the stable case ( $\Delta x = 0.01$  in the abstract form) gas velocity  $u$  and sound  $c$  were evaluated on a stable temperature profile, after which the quantity  $\Delta t$  was calculated. Boundary points were calculated to five places. Calculation was stopped when the distribution of all quantities became close to their final stable distribution.

## 5. Evaluation of the Results.

1°. First let us examine the manner in which transition for  $k = 6.17$  occurs, i.e., from the stable regime corresponding to  $K_4 = 0.1447$  to the new stable regime corresponding to  $K_5 = 0.0935$  (the remaining numerical parameters are as in 2° and 3°).

In Figure 2a and 2b, distances are laid out along the axis of the abscissa from the channel inlet to the inlet of the jet, and point  $x = 1.0$

corresponds to the inlet of the channel. Abstract pressure (Figure 2a) and temperature (Figure 2b) are laid out along the ordinate axis. A step along the coordinate is  $\Delta x = 0.01$ ; a step in time is  $\Delta t = 0.0075$ . The solutions are recorded at various moments in time. The time scale  $\Delta T = 0.3075$ , i.e., the curve indicated by the number 3, is the solution at the moment  $3\Delta T$  (several of the interim curves are not drawn in so as not to confuse the illustration).

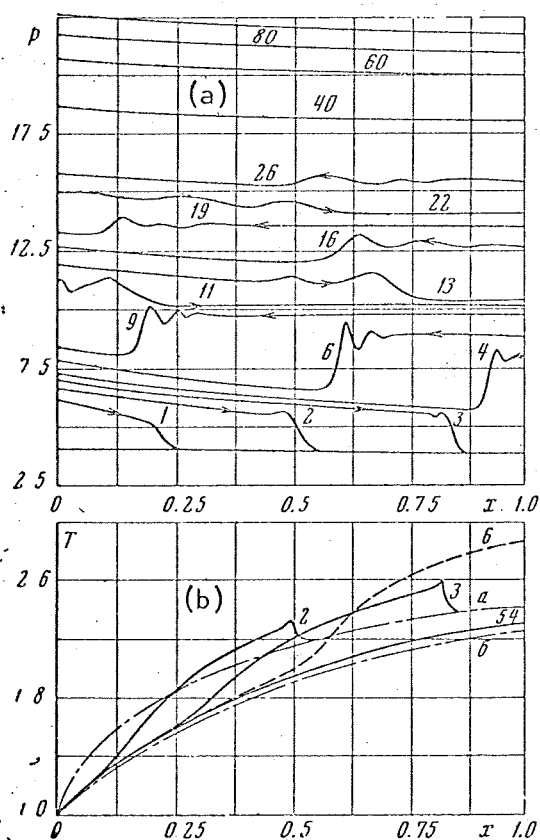


Figure 2.

is  $\Delta p/p_1 = 0.4$  (the ratio of pressure drop along the wave front to pressure in the undisturbed region). In curve 2 we find a depression. This tells of the appearance of a rarefaction wave arising as a result of the drop-off in the developing detonation.

Figure 2b (see curves 2 and 3) shows that heating of the gas by the shock wave is significant. We will evaluate the amount of temperature increase

The upper curve in Figure 2a is the final stable pressure profile ( $K = K_5$ ), the lower is the initial stationary pressure profile ( $K = K_4$ ). The time at which the new dispersion of oxidizer is established at the channel entrance equals  $\Delta T$ .

From the graphs it can be seen that after a change in dispersion of the oxidizer a shock wave begins to spread along the channel (in all figures the direction of wave distribution is indicated by an arrow), which upon reaching the nozzle is reflected from it and begins to spread back in the opposite direction, after which it reflects from the left boundary, etc. Its initial intensity

of the gas along the wave front at moment  $3\Delta T$ . Knowing  $\Delta p/p_1$ , from the Rankine-Gugonio correlation, we find that the ratio of gas temperature behind the shock wave to temperature in the undisturbed region equals 1.08. This corresponds to the ratio of these temperatures calculated for curve 3 in Figure 2b. Note that gas temperature at the channel end in the initial stable state is higher than gas temperature at the final stable state by 1.07 times (curves denoted by letters a and b are the initial and final stable distributions); however, because of gas heating by the shock wave, its temperature may be higher than originally. Upon reflection of the wave from the jet (Figure 2a, curve 6) a bottleneck of gas at higher temperature is formed (Figure 2b, curve 6). Then it begins to settle down slowly as the gas exits /39 through the jet. Temperature gradually decreases to stable corresponding to  $K = K_5$  (Figure 2b, curve 54).

The shock wave disperses to the left boundary with a velocity approximately two times less (relative to the channel wall) in comparison to the dispersion rate of the wave towards the jet. This is explained by the fact that the wave is moving in the direction opposite the direction of gas flow. The velocity of the shock wave relative to the wall is twice the speed of sound (evaluation per curves 2 and 3 in Figure 2a).

Reflection of the shock wave from the boundaries resembles reflection from solid walls. This is explained by the fact that the gas velocity in the channel is insignificant; therefore, in the time of reflection of the wave from the boundary, only an insignificant part of it manages to pass into the jet.

Upon reflection of the shock wave from the jet a small second hump is formed in its profile, apparently associated with the generation of a wave of rarefaction during reflection from the jet.

The shock wave attenuation which is observed in Figure 2a occurs mainly in amplitude. Attenuation of the wave is accompanied by erosion of its front. Reduction of wave intensity takes place because:

- a) a portion of the gas at the time of reflection manages to enter the jet;
- b) interaction of compression and rarefaction waves occurs;
- c) the wave is dispersed in a non-uniform medium (particularly after being reflected from the jet, the wave disperses in gas whose pressure increases as  $x$  decreases).

As seen from Figure 2a, attenuation of the wave in this case is quite significant during interaction with the gas being fed into the channel (curves 6 and 9), i.e., for the third reason.

Attenuation time of the wave (here is meant a noticeable reduction in its intensity) and transition to a new stationary regime will be given below.

After attenuation of the shock wave a gradual climb in pressure takes place almost to the final stable distribution because of the distribution along the channel of a low-intensity compression wave (they are therefore not visible on the graph). Besides the gradually diminishing wave arising at the initial moment, these waves are generated in the same place where the gas, entering the channel at moment  $t = 0$ , compresses the gas being expelled by them.

2°. Figure 3a illustrates the distribution of pressure along  $x$  at various moments in time for  $k = 0.5$ , i.e., for the transition from a stationary mode with  $K = K_1 = 0.0906$  to the mode corresponding to  $K = K_3 = 0.1070$  (the /40  
remaining numerical parameters are as in 1°, paragraph 3). The shift in time  $\Delta t = 0.01$  along coordinate  $\Delta x = 0.01$ , for which scale of time the curves are indicated, is  $\Delta T = 0.41$ . The time for establishing the new dispersion of oxidizer equals  $\Delta T$ . The upper curve is the stable distribution of pressure for  $K = K_1$ , and the lower is for  $K = K_3$ .

After the change in oxidizer consumption a simple rarefaction wave starts to spread in the channel and is reflected in turn first from the left and then from the right boundary.

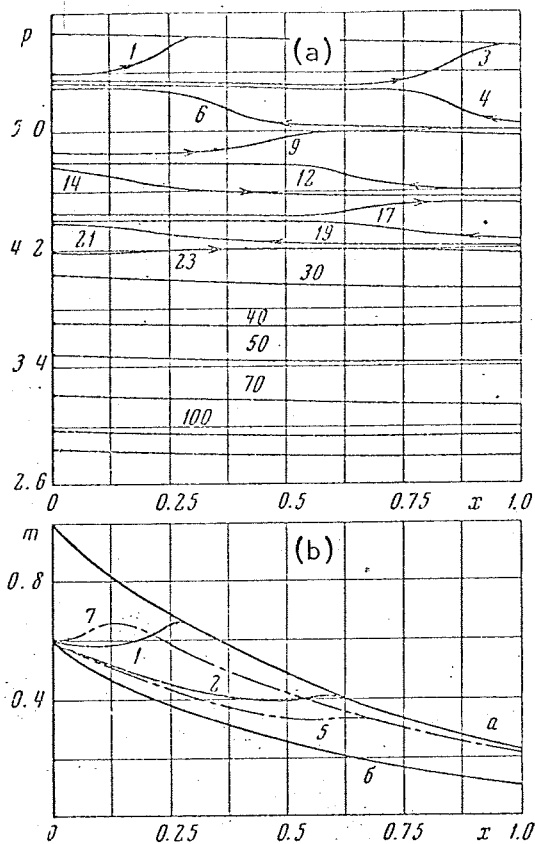


Figure 3.

temperature falls below the stable value corresponding to  $K = K_1$ , and then starts to increase slowly, approaching the final stationary distribution with  $K = K_3$ .

Insofar as transitory processes are related to dispersion of the shock wave (or rarefaction wave) along the channel, it is clear that combustion in the channel also is of a wave form. This is seen from Figure 3b, which illustrates the initial ( $K = K_1$ ) and final ( $K = K_3$ ) distribution of mass velocity of combustion  $m(x)$  (they are indicated by letters a and b, respectively), and also the instantaneous distribution of  $m(x)$  up to the moment of reflection of the wave from the channel entrance for several moments in time (time scale as in Figure 3a). The dot-dash curves correspond to wave reflections from the jet. Note that during stable combustion the maximum fuel

Intensity of the wave is not significant; temperature and concentration disturbances are carried through with the gas flow.

Reflection from the boundaries takes place as from a solid wall, i.e., out of phase with the arriving wave. As in case 1° at this point, the rarefaction wave gradually diminishes, and the wave front dissipates. In this case the wave also is dampened because it is mechanically unstable and the distribution of values in it become increasingly smooth with the passage of time.

The temperature behavior of the gas at the channel end is interesting. After the first reflection of the rarefaction wave from the jet, gas

consumption takes place at the channel inlet, since the behavior of the function  $m(x)$  is determined by the distribution of concentration (flow changes insignificantly).

In conclusion let us examine Figure 4, in which the value of pressure in the channel shear section  $p_l$  is plotted as a function of time. Curve 3 reconstructs case 1° for this point, curve 2 for case 2°, while curve 1 is for case  $k = 1.5$  (transition from the stable regime with  $K = K_1$  to the regime with  $K = K_2$ ). The latter case is associated with formation of the compression wave (its intensity is  $\Delta p/p_1 = 1/20$ ).

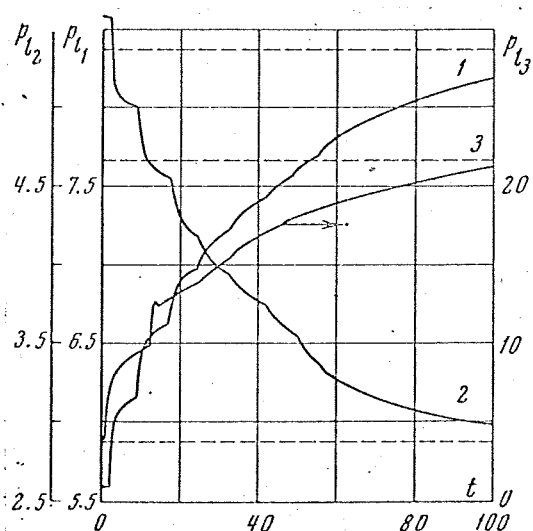


Figure 4.

The scale along the axis of the abscissa in Figure 4 is the following: point 100 corresponds to the moment  $t = 41$  for curves 1 and 2, and  $t = 30.75$  for curve 3.

Pressure value along the channel shear section changes abruptly when the shock wave (or rarefaction wave) reaches the jet. As the wave dampens, the value of these jumps decreases with the passage of time and toward the end

of the process a smooth transition to the final stable value takes place.

In Figure 4, the lower dashed line is the final static value for curve 2, the center one for curve 3, and the upper one for curve 1. Extrapolating curves 1, 2, and 3 to the intersection with the corresponding straight lines, we obtain the precise time of transition to the new stable regime. For curves 1 and 2,  $t_1 = 57.40$ ; for curves 3,  $t_1 = 31.36$ . This result is substantially different from the evaluated time of evacuation (or filling), calculated by stable distribution. Damping time of pressure pulsations comprises about  $1/3$  the time of transition to the new stable regime for curves 1 and 2 and  $1/2$  the transition time for curve 3.

The system of calculating transitory regimes proposed in the present work is based on supposition of a diffusion mechanism of solid fuel combustion, which is realized if there is an abundance of oxidizer in the channel, and the Reynolds number defining the combustion rate is sufficiently small. The specifics of this case consist in the fact that the combustion rate does not depend in any direct way on pressure.

As the Reynolds number increases, accompanied by an intensification of the combustion process, more intensive disturbance of the gas occurs in each cross section of the channel, and transition from the diffusion regime of combustion to the kinetic occurs, where the characteristic chemical reaction time is comparable to intermixing time. Combustion rate in this case is a function of pressure corresponding to kinetic chemical reaction, while the combustion regime in the channel itself is similar in large degree to combustion in a homogeneous chemical reactor. It is not excluded that the presence of a clear dependence of combustion rate on pressure can be led to occurrence of thermo-kinetic vibrations in the channel because of the inverse relationship between combustion rate and the gas exhaust through the jet, which is also pressure-dependent.

A supplementary effect can arise when examining restructuring of the thermal layer in the solid substance, leading to a change in the time of effective heat of combustion in the fuel. Consideration of the character of the thermal layer during the transitory regime is also substantial during diffusion combustion when the evacuation time is comparable to the restructuring time of the thermal layer. This effect was not considered in the present work in order to simplify calculation. In order for the allowance of the quasistability of the thermal layer to be vindicated in practice, the capacity of the fuel channel must be sufficiently high; in this case the burned layer will have time to follow the state of gas flow in the channel.

There is also some interest in solving the problem of transitory regimes in the case where oxidizer is not in sufficient supply in the channel. Along a certain length of channel, the oxidizer is completely consumed, while in the remaining part of the channel fuel ablation occurs along with combustion, under the effect of hot combustion products.

/41



We note in conclusion that the system of equations (2.3) can be solved by orienting all equations to  $x$ . In this case the solution does not take into consideration the gas-dynamic picture of phenomena having a substantial effect on average characteristics of the transitory regime. In particular, the values for time obtained using this approach for transition from one stable regime to another are considerably different from the real values obtained by numerical integration of the dynamic system of equations.

The authors thank L. A. Chudov for valuable consultation.

## REFERENCES

1. Zel'dovich, Ya. B., "Combustion Theory of Powders and Explosives," *ZhETF*, Vol. 12, No. 11, 12, 1942.
2. Zel'dovich, Ya. B., "Stability of Powder Combustion in a Semi-enclosed Volume," *PMTF*, No. 1, 1963.
3. Zel'dovich, Ya. B., "Combustion Rate of Powder Under Changing Pressure," *PMTF*, No. 3, 1964.
4. Novozhilov, B. V., "Transitory Processes During Powder Combustion," *PMTF*, No. 5, 1962.
5. Istratov, A. G., V. B. Librovich, and B. V. Novozhilov, "An Approximation Method in Dynamic Combustion Rate Theory," *PMTF*, No. 3, 1964.
6. Novozhilov, B. V., "Average Combustion Rate of Powder Under Harmonically Changing Pressure," *Fizika goreniya i vzryva*, No. 3, 1965.
7. Leypuskiy, O. I., V. I. Kolesnikov-Svinarev, and V. N. Marshakov, "Dynamic Combustion Rate of Gunpowder," *Dokl. AN SSSR*, Vol. 154, No. 4, 1964.
8. Barrer, M., A. Zhomott, B. F. Bebek, and Zh. Vandernkerkhofe, *Raketnye dvigateli*, [Rocket Engines], Oborongiz Press, Moscow, 1962.
9. Marxman, G. and M. Gilbert, "Turbulent Boundary Layer Combustion in the Hybrid Rocket," IX Sympos. (Internat.) on Combustion, New York--London, *Acad. Press*, 1963.
10. Librovich, V. B., "Ignition of Solid Fuels," *PMTF*, No. 2, 1968.
11. Rubin, E. L. and Z. Burstein, "Difference Methods for the Inviscid and Viscous Equations of a Compressible Gas," *J. Comput. Phys.*, Vol. 2, No. 2, 1967.

Translated for the National Aeronautics and Space Administration under contract No. NASw-2037 by Techtran Corporation, P. O. Box 729, Glen Burnie, Maryland, 21061.